Available online at www.sciencedirect.com
ScienceDirect
Acta Biomaterialia 3 (2007) 139–149
Acta BIOMATERIALIA
www.actamat-journals.com

Jumbo squid beaks: Inspiration for design of robust organic composites

Ali Miserez [a], Youli Li [b], J. Herbert Waite [c], Frank Zok [a,*]

[a] *Materials Department, University of California, Santa Barbara, CA 93106, USA*
[b] *Materials Research Laboratory, University of California, Santa Barbara, CA 93106, USA*
[c] *Department of Molecular, Cell and Development Biology, University of California, Santa Barbara, CA 93106, USA*

Received 20 July 2006; received in revised form 8 September 2006; accepted 15 September 2006

Abstract

The hard tissues found in some invertebrate marine organisms represent intriguing paradigms for robust, lightweight materials. The present study focuses on one such tissue: that comprising the beak of the jumbo squid (*Dosidicus gigas*). Its main constituents are chitin fibers (15–20 wt.%) and histidine- and glycine-rich proteins (40–45%). Notably absent are mineral phases, metals and halogens. Despite being fully organic, beak hardness and stiffness are at least twice those of the most competitive synthetic organic materials (notably engineering polymers) and comparable to those of *Glycera* and *Nereis* jaws. Furthermore, the combination of hardness and stiffness makes the beaks more resistant to plastic deformation when in contact with blunt abrasives than virtually all metals and polymers. The 3,4-dihydroxy-L-phenylalanine and abundant histidine content in the beak proteins as well as the pigmented hydrolysis-resistant residue are suggestive of aromatic cross-linking. A high cross-linking density between the proteins and chitin may be the single most important determinant of hardness and stiffness in the beak. Beak microstructure is characterized by a lamellar arrangement of the constituents, with a weak interface that promotes crack deflection and endows the structure with high fracture toughness. The susceptibility of this microstructure to cracking along these interfaces from contact stresses at the external surface is mitigated by the presence of a protective coating.

Keywords: Hard tissue; Chitin; Histidine; DOPA; Abrasion

1. Introduction

Nature's strategy to create structures that pierce, inject, crush or rasp in both vertebrate and invertebrate species usually involves biomineralization [1,2]. Human teeth, for instance, contain about 95 wt.% mineral in the external enamel layer and 70 wt.% mineral in the softer dentin interior. Biomineralization is also the common strategy employed by molluscs for their protective shells [3–5].

Despite its prevalence in biological materials, biomineralization is not the only strategy available to produce structures that perform a biting function [2]. The jaws of the polychaete worm *Glycera*, for instance, are composed predominantly of a robust cross-linked network of organic molecules, notably melanin and proteins, with only small amounts (5–10%) of the Cu-based mineral atacamite [6]. Despite the low mineral content, the resistance to abrasion, characterized by the performance index H^3/E^2 (H being hardness and E the Young's modulus), lies between those for dentin and enamel. Jaws of the polychaete marine worm *Nereis* [7] and the mandibles of some arthropods [8–10] are altogether devoid of mineral, yet they too exhibit good abrasion resistance [11]. In the latter cases, hardening is correlated with the presence of metal ions, usually Zn^{2+}. Their concentrations attain levels of about 3% of dry mass in *Nereis* jaws and 15% in ant mandibles [9,10].

The focus of the present article is on another hard but unmineralized biomolecular material: the beaks of the jumbo squid (*Dosidicus gigas*, Cephalopoda). Squid beaks

* Corresponding author. Tel.: +1 805 893 8699.
E-mail addresses: zok@engineering.ucsb.edu, flowers@engineering.ucsb.edu (F. Zok).

1742-7061/$ - see front matter © 2006 Acta Materialia Inc. Published by Elsevier Ltd. All rights reserved.
doi:10.1016/j.actbio.2006.09.004

are impressively robust structures that play a crucial role in feeding. The closure forces exerted by the mandibular muscles of some species are large enough to crush the shells of gastropods [12,13]. Moreover, the presence of intact beaks in the stomachs of squid predators indicates a high resistance to proteolysis [14–16].

Knowledge about cephalopod beaks has emerged largely from ecological and population studies [16–23], the growing interest from the fish industry [22,24–26] and interest in the dietary habits of their predators [15,16,27,28]. Morphometric characteristics of beaks are summarized in the handbook of Clarke [15]. Some of these features are depicted in Fig. 1. The focus here is on the rostral (tip) region, since this is unmistakably the hardest part. In contrast, the back of the lateral wall and the wing have mechanical characteristics similar to soft cartilaginous tissues with a hydrogel-like texture. Their properties also appear to be correlated with coloration, hardness increasing with level of pigmentation [17,20,29].

The limited literature suggests that cephalopod beaks consist of chitin fibers (poly-*N*-acetyl-D-glucosamine, a cellulose-like polysaccharide), embedded within a protein matrix [17,22,23,29–31]. Alkali deproteinization treatments of *Octopus vulgari* beak rostra indicate chitin levels of about 6–7 wt.% [29]. Enzymatic studies on the beaks of *Loligo* species suggest higher levels, at about 20% [32]. These studies also indicate that the beaks are devoid of minerals. The presence of metal ions or halogens in any form has not been reported.

The present interest in the beaks of jumbo squid is motivated in part by their unusually large size. This feature facilitates fracture toughness testing using specimen geometries that conform to established standards and thus obviates the difficulties associated with the use of alternate methods, notably indentation. Although appropriate for use on hard materials (ceramics and glasses, for instance), indentation has proven to be ineffective for biological materials, because of problems in generating cracks in soft materials [33]. Indeed, the paucity of fracture toughness data for these materials is a direct consequence of their low hardness as well as the availability of only small samples.

2. Materials and methods

2.1. Experimental species

Squid beak samples were provided by the Centro de Investigaciones Biológicas del Noroeste, La Paz, Mexico. The beaks were freshly extracted from *Dosidicus gigas* captured in the Gulf of California, washed with ethanol, and preserved in distilled water at 4 °C until sectioning. For all experiments except those involving X-ray measurements, the beaks were initially cut along their plane of symmetry using a low speed diamond saw, as illustrated in Fig. 1a.

3. Structure characterization

Beak microstructures were characterized by optical and scanning electron microscopy (SEM). Both longitudinal and transverse sections (relative to the long axis of the beak) were prepared by either standard mounting and polishing procedures (to 0.25 μm finish) or by ultramicrotomy.

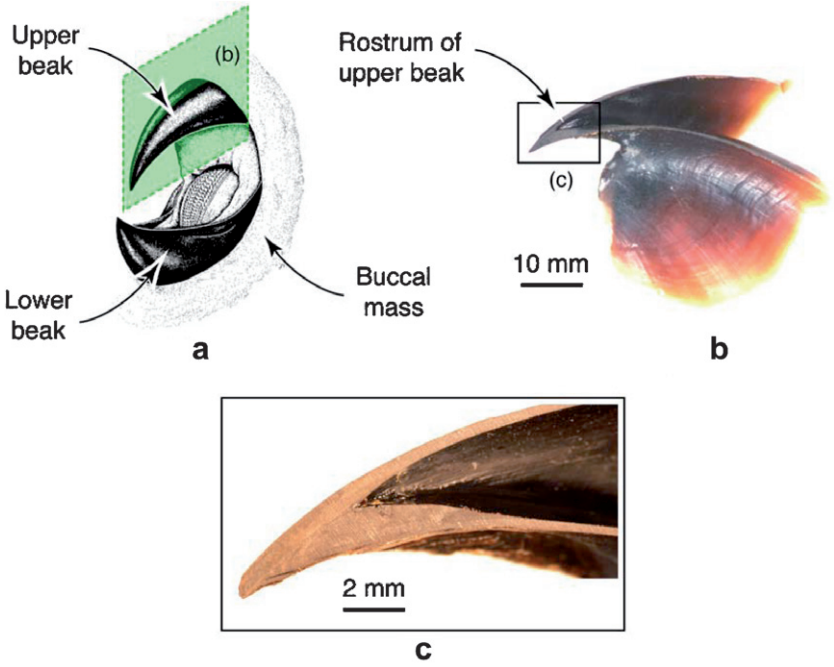

Fig. 1. (a) Schematic illustration and (b, c) optical micrographs of a longitudinal cross-section through the tip of the upper beak. Schematic adapted from http://seawifs.gsfc.nasa.gov/OCEAN_PLANET/HTML/squid_eat.html.

Contrast was obtained using cross-polarizers and Nomarski filters.

X-ray diffraction studies were carried out on near-tip samples, approximately 2 cm × 2 cm in size, using a wide angle X-ray scattering (WAXS) spectrometer equipped with a Cu rotating anode X-ray generator (Rigaku UltraX18), a double-focusing graded multilayer monochromator and a Mar345 image plate area detector. The beam size at the sample position is ~1 mm × 1 mm. Diffraction patterns were corrected for background by acquiring a blank pattern under otherwise identical operating conditions. Larger scale structural ordering was probed by small-angle X-ray scattering (SAXS) using a custom diffractometer capable of probing length scales up to 60 nm. Scans were acquired at various locations along the upper beak: close to the tip as well as near the middle. SAXS patterns were integrated over the azimuth using the Fit2D software [34].

3.1. Chemical analysis

Amino acid (AA) composition and total protein content were obtained by AA analysis. Small sections from the beak rostrum were freeze-dried, weighed and placed in hydrolysis tubes with 6 M HCl and 5% phenol as antioxidant. The tubes were vacuum-sealed and heated at 110 °C for three days. The supernatant was then separated from the solid residue by centrifugation, flash-evaporated and analyzed in a ninhydrin-based Beckman Autoanalyzer (Beckman-Coulter, Fullerton, CA). The AA concentrations were calibrated using external standards. To assess whether full hydrolysis had been achieved, the solid residue was washed and rehydrolyzed in a fresh 6 M HCl/5% phenol solution in vacuo for an additional 24 h and the resulting supernatant was similarly separated, flash-evaporated and analyzed. The latter step proved unnecessary, however, as the additional ninhydrin-positive material released was <0.01% of that following the initial hydrolysis. The protein mass fraction was estimated from the total AA mass and that of the initial sample.

To separate 3,4-dihydroxy-L-phenylalanine (DOPA) and other catecholic compounds, beak samples were hydrolyzed for 2 h and, following flash evaporation, bound to a phenyl boronate affinity column [35] and washed with 3 column volumes of 0.1 M phosphate (pH 7.5) before eluting with 5 vol.% acetic acid. To extract and identify free catechols, beak samples were crushed in liquid N_2, homogenized in 5% acetic acid and run through the phenyl boronate column. The AA compositions of the eluting fractions were then analyzed with the Beckman Autoanalyzer as above.

The chitin mass fraction was obtained from mass changes of freeze-dried beak samples following a deproteinization/depigmentation treatment [36]. One treatment cycle consisted of immersing in aqueous KOH at room temperature overnight followed by a 2 h soak in chlorite solution at 70 °C. After each soak, the suspension, containing the supernatant and micrometer-sized chitin particles, was extracted and separated by centrifugation. The resulting particles were freeze-dried and weighed. The solid portions remaining after each treatment cycle were subjected to additional treatment cycles until no additional solid particles were released. The chitin mass fraction was obtained from the ratio of the total solids mass (that due to both the residue and the fine particles) to the initial sample mass. To assess whether deproteinization had progressed to completion, the solid residue was hydrolyzed according to the aforementioned procedures for AA analysis and the AA content measured. In this case, the only significant spectral peak matched that of glucosamine hydrochloride (GA HCl): the hydrolysis product of chitin when subjected to 6 M HCl. The results confirmed that full deproteinization had indeed been achieved and that the solid residue was purified chitin. Further confirmation of the latter result was obtained from comparisons of X-ray powder diffraction patterns for the remaining powder and those for an α-chitin standard (purified from crab shells, Sigma–Aldrich) and a β-chitin powder (from a *Dosidicus gigas* pen).

3.2. Mechanical properties

Mechanical properties were assessed by nanoindentation. Samples for indentation were prepared as those for microscopy, notably either by polishing or by ultramicrotomy. Indentation tests were performed in an instrumented nanoindenter (Triboscope, Hysitron, Minneapolis, MN). To facilitate hydration, test samples were placed in a glass crucible. Tests were first performed in ambient air using a cube-corner diamond tip. The properties of the near tip region were mapped by performing a series of indentations in a two-dimensional array, spaced between 50 and 200 μm apart. A typical series contained about 200 indentations. The crucible was then filled with distilled water to a level approximately 2 mm above the height of the sample surface. The submerged samples were left undisturbed for at least 1 h prior to further testing. An identical series of indentations was performed on the submerged samples, but with the array offset by 20 μm with respect to the first set, to mitigate interactions between indentations. All indentations were performed at a loading rate of 1 mN/s to a peak of 4 mN, held at load for 10 s and unloaded at 1 mN/s. To ascertain hardness and modulus, the load–displacement response for each indentation was analyzed using the method of Oliver and Pharr [37]. The software package Origin (OriginLab Corporation, Northampton, MA) was then used to convert the data into hardness and modulus maps.

Fracture toughness measurements were made using single-edge notched tension (SENT) specimens. For this purpose, longitudinally oriented samples were extracted from the near tip regions of the beak using a sharp scalpel while keeping the sample hydrated. The samples were typically 5–8 mm wide and 20–30 mm long. To enable gripping, the sample ends were placed into a pair of aligned rectangular

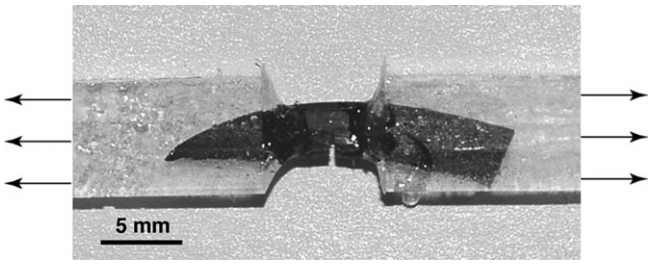

Fig. 2. Single-edge notched tensile specimen for fracture toughness measurement, embedded in epoxy tabs.

Teflon moulds and the mould cavities filled with epoxy. Once the epoxy had cured, an edge notch was cut into the sample at mid-section using a thin (200 μm) diamond blade. A typical test sample is shown in Fig. 2. Mechanical tests were performed in uniaxial tension in an MTS Bionix100 universal testing machine (MTS, Eden Prairie, MN) equipped with an environmental chamber. Tests were performed either in ambient air or submerged in water (following a 30 min soak). Fracture toughness, K_{Ic}, was calculated in accordance with

$$K_{IC} = \sigma_m \sqrt{\pi a} f(a/W) \quad (1)$$

where σ_m is the far-field tensile stress at fracture, a is the initial notch length, W is the width, and $f(a/W)$ is a non-dimensional function given in Tada et al. [38]. For selection of the appropriate form of $f(a/W)$, the boundary condition on the jaw portion of the test specimen was assumed to be one of a uniformly distributed tensile load. The validity of this assumption was assessed by comparing the fracture toughness values obtained on specimens of PMMA prepared in two ways. The first was identical to that used for the beaks, i.e. a small sample cast into epoxy ends. The second was a full-length SENT specimen (comparable to that of the epoxy ends) without a reduced area in the mid-section. The resulting fracture toughness values were essentially identical for the two geometries provided the function $f(a/W)$ was selected according to the uniformly loaded end condition. When the boundary condition was assumed to be one of uniform displacement, the latter results differed from one another by a factor of 2.

Fracture surfaces of the test specimens were subsequently gold-coated and examined in an SEM.

4. Results and analysis

4.1. Biochemistry

The AA composition of a near-tip beak sample (Fig. 3) was dominated by glycine (26%), alanine (14%) and histidine (about 10%). Other notable constituents detected were DOPA (at 45 min) and a broad peak at 40 min corresponding to glucosamine, as seen by comparing the sample with a hydrolyzed chitin standard. Although DOPA was typically detected at trace levels, up to 2 mol.% was present in samples subjected to shorter (2 h) hydrolysis times. Beaks contained no detectable free DOPA or any other type of catecholamine. The average AA compositions are summarized in Table 1. The total protein weight fraction was determined to be 40–45 wt.% dry as based on recoverable AAs following hydrolysis.

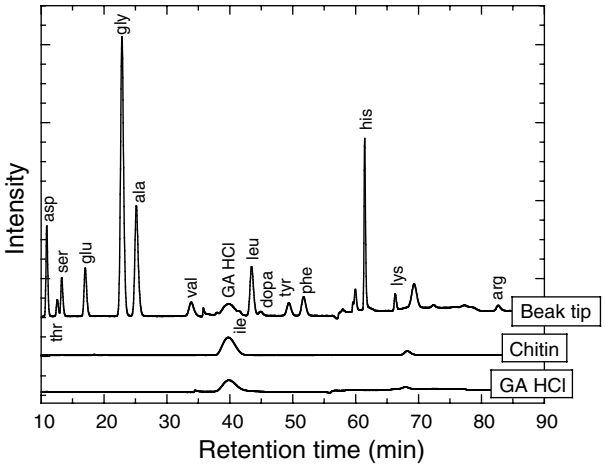

Fig. 3. Beckman spectra of a hydrolyzed beak, a glucosamine hydrochloride (GA HCl) control and a purified hydrolyzed chitin sample.

The X-ray powder diffraction spectra (Fig. 4) revealed that the only crystalline phase in the beaks was α-chitin, manifested by the intense peaks at $2\theta = 9$ and 19° (associated with the (002) and the combination of (101) and (004) reflections, respectively [39,40]) and the weaker peaks at 12, 23 and 27° (due to (012), (103) and (031) reflections). In contrast, the β-chitin exhibits only two broad peaks, at $2\theta = 8°$ and 19°. From the corresponding chemical analysis, the chitin mass fraction was estimated to be 15–20%. The EDS measurements revealed no detectable levels of metals or halogens. The nature of the remaining 35–40% of the beaks is unknown. A blackish insoluble

Table 1
Amino acid composition of beak rostrum after 24 h hydrolysis (averaged over five samples)

Amino acid	% residue
Aspartic acid (asp)	6
Threonine (thr)	2
Serine (ser)	3
Glutamic acid (glu)	5
Proline (pro)	1
Glycine (gly)	27
Alanine (ala)	15
Valine (val)	3
Isoleucine (ile)	5
Leucine (leu)	9
DOPA	<1
Tyrosine (tyr)	3
Phenylalanine (phe)	5
Histidine (his)	11
Lysine (lys)	1
Arginine (arg)	1

The DOPA content is higher (~2 mol.%) for shorter hydrolysis times.

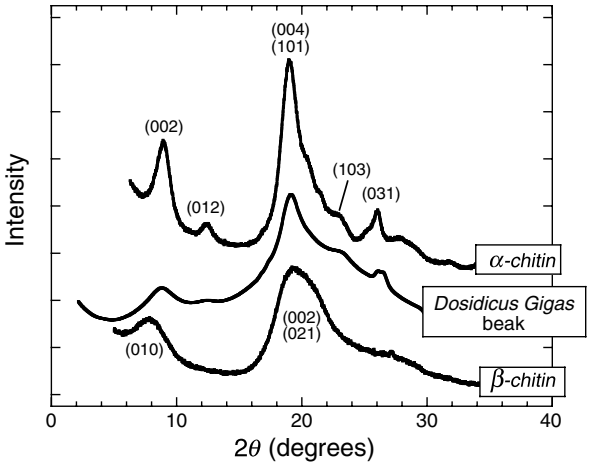

Fig. 4. Wide angle X-ray diffraction spectra for the jaw beaks, α-chitin (crab shell) and β-chitin (*Dosidicus* pen). Diffraction angles determined using lattice parameters provided by Carlström [63] for α-chitin and Blackwell [64] for β-chitin. α-chitin: orthorhombic cell, $a = 4.74$ Å, $b = 10.32$ Å, $c = 18.86$ Å; β-chitin: $a = 4.85$ Å, $b = 10.38$ Å, $c = 9.26$ Å, $\theta = 97.5°$. In both cases, b is the orientation of the fiber axis.

powder remained after extensive hydrolysis and represented about 10 wt.% of the initial dry weight.

4.2. Structure

In the near-tip regions, the beak material exhibits a largely lamellar microstructure. The pertinent features are revealed both in optical micrographs of microtomed sections (Fig. 5) and on the fracture surfaces (Figs. 6 and 7). The lamellae are typically 2–3 μm thick. They are aligned parallel with the long axis of the beak (with alignment planes "pointing" to the jaw tip) and oblique to the beak surfaces. The inclination angle relative to the surfaces varied from 90° (Fig. 5(a)) to about 50° (Figs. 6a and 7). Some lamellar curvature is usually observed across the thickness. The lamellae extend entirely to the inner beak surface, but terminate about 50–100 μm from the external surface, where they impinge on a protective coating (Fig. 7). The coating does not exhibit any discernible microstructural features when viewed by either optical or scanning electron microscopy (Figs. 5a and 7a). Anecdotal observations of the interaction of water with the two surfaces suggest that the coating serves as a hydrophobic sealant. That is, when placed on the external surface, water forms droplets with a high contact angle and does not penetrate into the tissue; in contrast, water readily penetrates the tissue from the internal surface. When viewed at low magnifications, the fracture surfaces seemingly display lamellae-like features at a coarser scale, with spacing of about 50 μm (Fig. 7). Upon closer examination, however, these are found to be a consequence of delamination between packets of many lamellae, typically 20–30. The regularity of the layered packets suggests the presence of periodic microstructural heterogeneities that promote delamination and possibly enhance the resistance to crack propagation, as manifested in the fracture toughness (below). In the absence of corroborating evidence, however, this notion remains rather speculative.

Representative SAXS patterns and the corresponding integrated intensities for samples both from the near tip region and near the beak middle are shown in Fig. 8. At the tip, the patterns are anisotropic, with the short axis aligned with the external beak surface. The inference is that the scattering particles are elongated and preferentially aligned at the tip. In contrast, the patterns appear isotropic in the middle sections, suggesting random orientation of the particles The characteristic dimensions of the scattering particles were ascertained using Guinier's analysis [41,42]. The intensity I is predicted to vary with the scattering vector Q in accordance with $\ln(I/I_0) = -Q^2R_g^2 3$ where $Q = 4\pi\sin\theta/\lambda$, λ is the wavelength, 2θ is the scattering angle, R_g is the particle radius of gyration and I_0 is a reference intensity. In the low angle region, all plots of ln I vs. Q exhibit two linear regimes: one at very small angles ($Q^2 < 0.01\ \mathrm{nm}^{-2}$) and the other at larger angles ($Q^2 = 0.04$–$0.1\ \mathrm{nm}^{-2}$). Furthermore, the sizes of the scattering particles from each of the two domains are the same both in the tip and middle regions, as manifested in the similarities in the slopes of the curves. The inferred radii of gyration are $R_g = 25$–30 nm and $R_g = 5$–7 nm. Finally, an attempt was made to fit the entire curve, using the particle sizes inferred from the two limits. The quality of this fit at intermediate Q values is only moderate, suggesting the presence of a spectrum of sizes between the two limiting values.

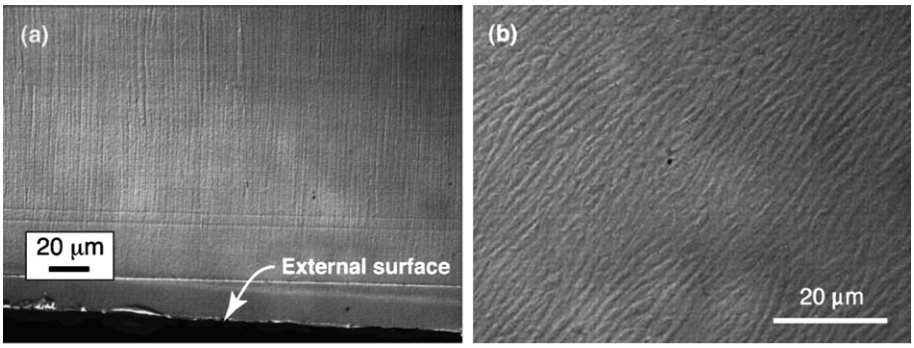

Fig. 5. Optical micrographs of (a) transverse and (b) longitudinal cross-sections (horizontal lines in (a) are scratches produced by the microtome blade).

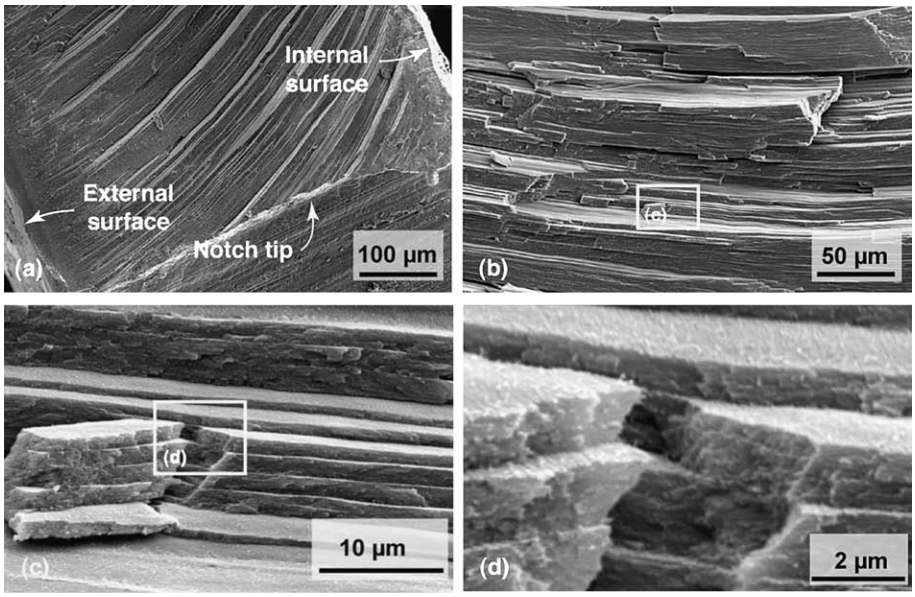

Fig. 6. Scanning electron micrographs of fracture surfaces showing the lamellar structure at progressively increasing magnifications.

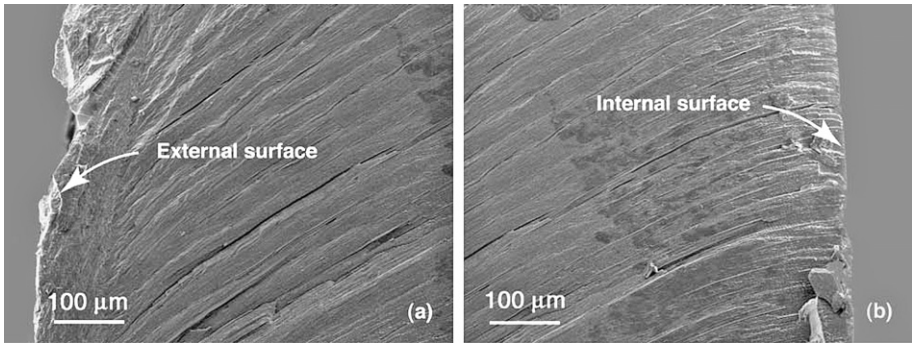

Fig. 7. Fracture surfaces showing (a) termination of lamellar structure 50–100 μm from the external surface and (b) continuation of lamellae to the internal surface.

4.3. Mechanical properties

4.3.1. Modulus and hardness

Typical modulus and hardness maps of transverse sections in the near-tip region both in air and under water are presented in Fig. 9. When dry, the average property values for this specific sample are $E = 8.7 \pm 0.6$ GPa and $H = 0.65 \pm 0.09$ GPa (from about 200 indents). When tested in water, the properties are reduced by about one-third: $E = 5.1 \pm 0.7$ GPa and $H = 0.43 \pm 0.14$ GPa. Although the spatial variations in properties are small, the hardness in the near-surface regions appears to be slightly higher than that in the middle. Tests on other samples revealed only small property differences from one beak to the next, with average values consistently in the range $E \approx 7$–9 GPa, $H \approx 0.6$–0.7 GPa (dry) and $E \approx 4$–6 GPa, $H \approx 0.3$–0.5 GPa (wet). The former (dry) values are remarkably similar to those recently measured on the jaws of both *Nereis* and *Glycera* worms [43].

4.3.2. Fracture toughness

The distributions of the fracture toughness are summarized in Fig. 10. There does not appear to be a statistically significant difference associated with the test conditions; the average values are $K_{Ic} = 3.2 \pm 1.5$ and 3.5 ± 1.1 MPa $m^{1/2}$ for dry and wet, respectively. The scatter is likely associated with (i) intrinsic property variations from beak to beak and (ii) deviations from the idealized geometry, due to the complex shapes of the beaks.

Alternatively, these results can be expressed in terms of critical strain energy release rates (or fracture energies) G_{Ic} via the Irwin relation

$$G_{Ic} = K_{Ic}^2/\bar{E} = K_{Ic}^2(1 - v^2)/E \quad (2)$$

where $\bar{E} = E/(1 - v^2)$ (known as the plane strain modulus) and v is Poisson's ratio (assumed to be 1/3). Combining this with the moduli measured by indentation, the corresponding fracture energies are $G_{Ic} = 1.5 \pm 1.1$ and 2.8 ± 1.9 kJ/m^2 for dry and wet conditions, respectively.

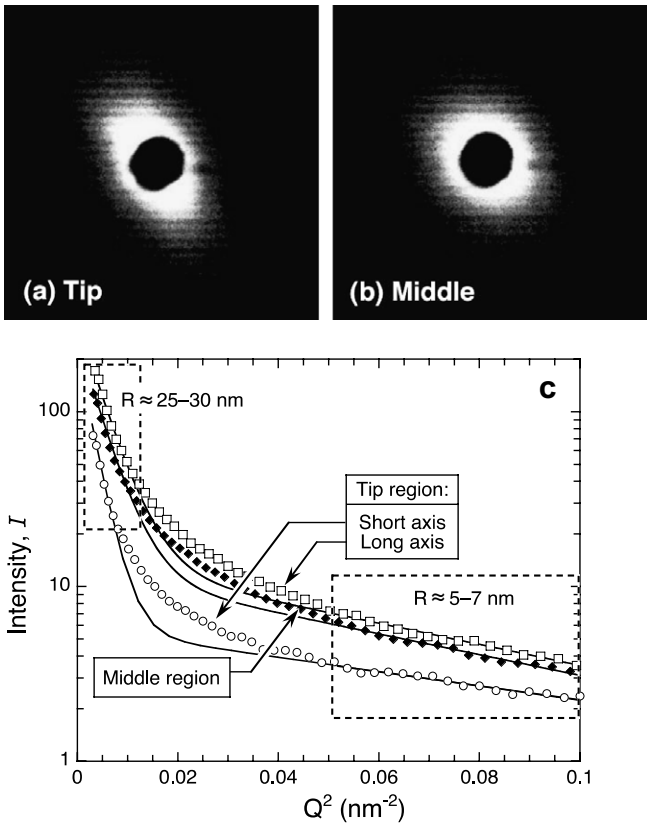

Fig. 8. SAXS patterns in the low angle region in (a) the near-tip and (b) the middle regions of the beak, as well as (c) integrated intensities and fits according to Guinier's analysis.

In this form, some effects of the test conditions emerge, although the large scatter precludes a definitive assessment.

5. Discussion

5.1. A perspective on properties

To provide a broader perspective, the hardness and stiffness of *Dosidicus* beaks were compared with those of common engineering materials, including polymers, metals and ceramics, as well as the jaws of *Glycera* and *Nereis* worms, dentin and enamel (Fig. 11a). When dry, the properties of the squid beak are essentially the same as those of the two worm jaws and exceed those of all engineering polymers by at least a factor of 2. In light of the fully organic nature of the squid beak, the latter result is particularly striking. Not surprisingly, however, their properties were lower than those of most metallic alloys and all ceramics.

5.2. Implications for abrasion resistance

In order to maintain functionality, the beak tip must not abrade excessively during contact with prey, food or other foreign bodies. A preliminary assessment of abrasion resistance can be made from the measured properties combined with an analysis based on contact mechanics. Without much loss in generality, the material (the beak in the present case) can be treated as a flat plate and the abrading material as a rigid solid of revolution with local curvature, $1/R$. The applied force P is taken to be normal to the contact site. The principal mechanical properties that dictate the local response are $\bar{E}$, H and G_{Ic}. Provided that the contact radius a is much smaller than R, the stress distributions are given by the well-known Hertzian solutions [44]. These distributions are combined with the appropriate failure criteria to ascertain the corresponding failure loads. Two failure modes are considered: (i) the onset of plastic deformation and (ii) the formation of cracks, prior to plastic deformation.

The normal load, P_y, for yielding is given by [44,45]

$$\frac{P_y}{R^2} = C_1\left(\frac{H^3}{\bar{E}^2}\right) \tag{3}$$

where C_1 is a constant of order unity. For hard and/or brittle materials, cracking precedes yielding. Cracks emanate from surface flaws just outside the contact circle, penetrate to a depth comparable to the contact radius a (following a conical trajectory) and then arrest. The critical load P_c to develop such a crack is [46]

$$\frac{P_c}{R} = C_2 G_c \tag{4}$$

where C_2 is a non-dimensional parameter of order 10^4 [47].

Comparative assessments of abrasion resistance of various materials can thus be made by plotting $H^3/\bar{E}^2$ vs. G_c. Fig. 11b shows such a plot. Here the critical loads for yielding are represented by a family of horizontal lines (defined by Eq. (3)) and those for cracking by vertical lines (Eq. (4)). Since either of the two processes constitutes the initiation of abrasive failure, the lower load is used to characterize abrasion resistance. To display this result, the vertical lines are truncated where they meet their horizontal counterparts, and vice versa, thereby yielding a family of L-shaped curves, one for each failure load. Materials with property data above and to the right of such a curve have higher critical loads. On this basis, the performance of the squid beak against a blunt abrasive is intermediate to dentin and enamel and comparable to the best engineering polymers and metals, but inferior to ceramics.

5.3. Biochemistry and structure

The presence of chitin, His-rich proteins and catechols (i.e. DOPA) in *Dosidicus* beaks suggests intriguing parallels with insect cuticles. All hard insect cuticles contain some chitin, with concentrations between 15% and 30% of dry weight [48]. Like cellulose, chitin is stiff in tension and, especially when oriented with the axis of loading, contributes to the reinforcement of the protein matrix. Beak proteins are glycine-, histidine- and alanine-rich. Overall, insect cuticles are also glycine- and alanine-rich [49]. Although the global histidine content of cuticles rarely stands out, the enrichment of histidine near the C-terminal

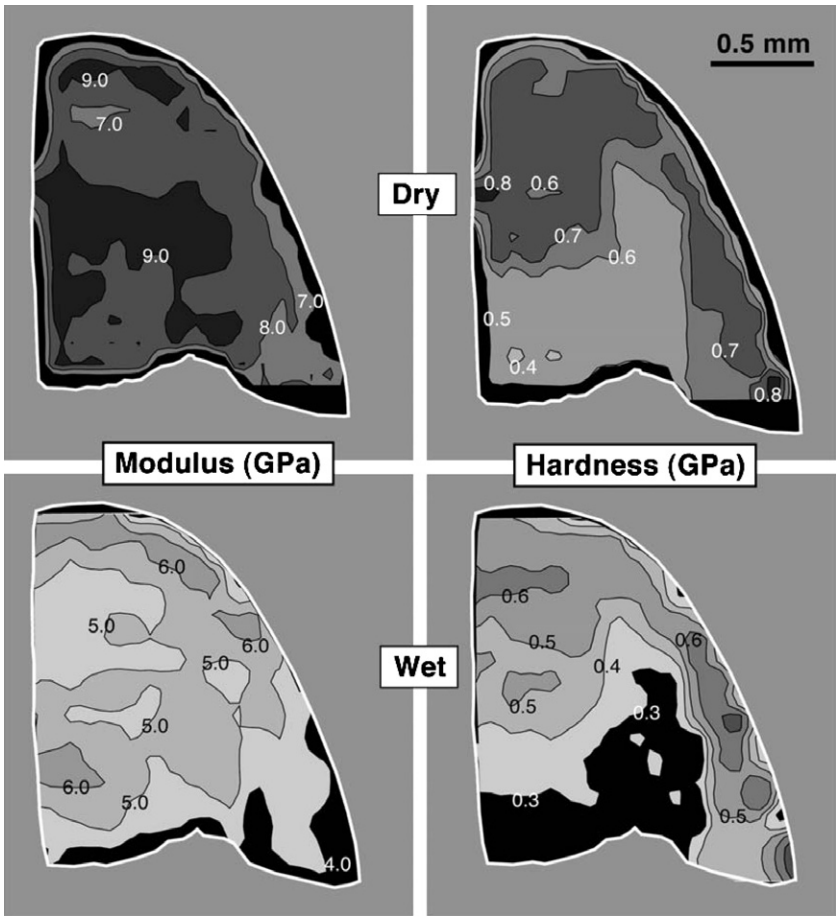

Fig. 9. Modulus and hardness maps in both wet and dry conditions for a transverse section situated about 2 mm from the tip of the beak. The white outlines represent the boundary of the beak cross-section.

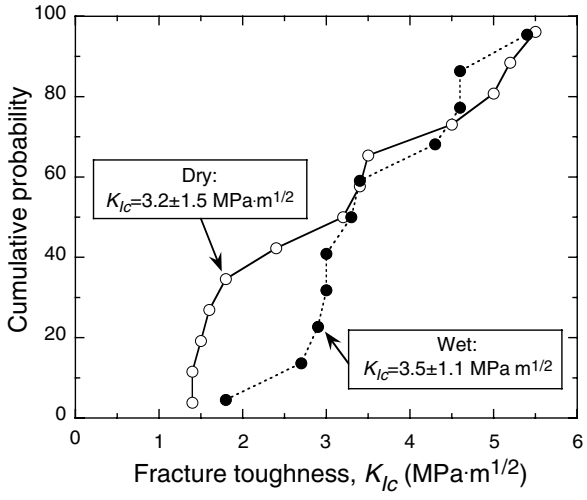

Fig. 10. Fracture toughness distributions for beaks in both dry and wet conditions.

region of cuticular proteins and its role as a sclerotizing agent have been emphasized [50,51]. Chitin is traditionally viewed as extensively H-bonded to cuticular proteins through histidyl residues to form stable glycoprotein complexes [31,50]. In more recent analyses of hydrolyzed insect cuticle, however, covalent cross-links of catechols coupled to both histidine and glucosamine (presumably from chitin) have been evident [51–54]. The abundance of histidine in *Dosidicus* beaks more closely resembles *Nereis* and *Glycera* jaw compositions than insect cuticle [55,56].

The presence of DOPA, a catecholamine, in *Dosidicus* beak is the third chemical feature reminiscent of insect cuticles. This similarity, however, must be approached with circumspection. During their formation, insect cuticles are permeated with low-molecular-weight catecholamines such as *N*-acetyldopamine and β-alanyldopamine. Following oxidation, the catecholamines polymerize to form a complex aromatic network [57]. In contrast to the low-molecular-weight catecholamines of insect cuticle, the DOPA in *Dosidicus* beak appears to be firmly tethered to protein; no directly extractable DOPA was detectable. This suggests that the DOPA in beak precursor proteins arises from tyrosine by post-translational modification, as it does in the sclerotization of other biological polymers such as byssal threads and egg capsules [58]. Oxidation of peptidyl-DOPA to quinone in the beak may contribute to both pigmentation and intermolecular cross-linking, particularly with histidine and cysteine residues [52,59], but these reactions remain to be demonstrated in the beak.

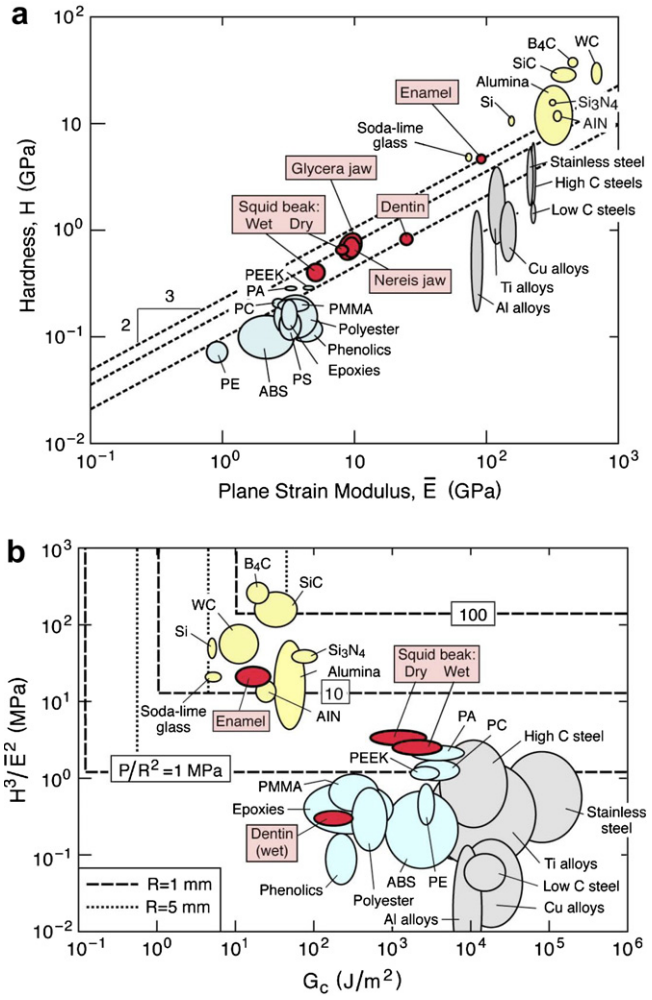

Fig. 11. Property maps showing (a) comparisons of hardness and stiffness of *Dosidicus* beaks with typical engineering materials and (b) critical loads for yielding and for cracking at contact with spherical rigid abrasives.

Perhaps related to DOPA is the significant unanswered question about the weight percentage beak composition. Assuming the protein to be 45 wt.% and chitin 20 wt.%, 35 wt.% remains unattributed. It is known with confidence that the unknown fraction contains no minerals, halogens or metal ions (data not shown). Despite the similarity of the protein compositions, the unknown weight percentage of the beak clearly distinguishes it from *Nereis* jaws, which contain significant levels of halogens and Zn ions [43], and *Glycera* jaws, which, apart from protein, contain atacamite, copper ions and melanin [6,55]. Neither worm jaw contains chitin. The black insoluble residue following exhaustive hydrolysis of *Dosidicus* beak is suggestive of the melanin of *Glycera* jaws. It constituted about 10 wt.% of the initial beak weight and hence accounts for about one-third of the unknown constituents.

Given the entirely organic composition of *Dosidicus* beak, a mechanistic explanation for the high stiffness and hardness would be very desirable. Histidine is a natural suspect since it is elevated in the compositions of several high-impact structures, including polychaete jaws [55,56] and nematocyst stylets [60]. Recently, Broomell et al. [43] showed that in *Nereis* jaws hardness and stiffness were directly related to Zn ions, which presumably cross-link the histidine-rich proteins by the formation of multiply liganded coordination complexes, e.g. $Zn(His)_3Cl$ [7]. Similar strengthening mechanisms may be operative in the mandibles and fangs of arthropods [9,10], but are not possible in *Dosidicus* given the absence of metals. The hardness and stiffness of the *Glycera* jaw derive some benefit from the continuous melanin matrix and in the near-surface regions are further elevated by small amounts of atacamite fibers and Cu^{2+} ions [55,61]. Here again, there are no obvious insights for *Dosidicus* beak. We are left to propose that hardness and stiffness in *Dosidicus* beak may be a result of high-density DOPA-derived cross-linking and the black powdery residue following hydrolysis. This is consistent with preliminary tests using Arnow's stain, which specifically stains DOPA, showing an accumulation of DOPA-proteins in the slightly pigmented region of the cartilage directly adjacent to the harder portion of the beak. That is, there is a direct correlation between the onset of hardening and the presence of DOPA. Further investigations of this are currently underway [62].

The organization of the constituents into lamellae represents an additional important characteristic of the beak structure and is likely the key determinant in the fracture toughness. In order to achieve high toughness, the lamellae must be separated by a weak interface. The toughness is a consequence of crack deflection along this interface, followed by crack re-nucleation in neighboring lamellae. This deflection is evident on the fracture surfaces of the beak specimens. To first order, the fracture energy is proportional to the spatial extent of deflection, which, in turn, scales with the lamellae thickness.

The benefits of the lamellar microstructure, however, are only obtained when cracks propagate oblique or normal to the plane of the lamellae. In the presence of tensile loads transverse to this plane, cracks can propagate relatively unimpeded along the interfaces between the lamellae. Thus, if the lamellar structure of the beaks were to persist through the entire wall thickness to the external surface, the beak would be susceptible to through-thickness cracking during application of contact forces. Interestingly, this problem is mitigated by the presence of a thin (50–100 μm), relatively homogeneous coating on the external surface. The implication is that the coating serves at least two functions: (i) it protects the interior lamellar structure from the near-surface stresses that arise during contact with external bodies; and (ii) it prevents ingress of water (and perhaps other species) into the jaw, as noted earlier.

6. Conclusions

The main constituents of *Dosidicus* squid beaks are chitin fibers (5–35 nm in size) and His- and Gly-rich proteins. Notably absent are any mineral phases and metals. Despite being fully organic, the beaks exhibit impressive

mechanical properties. When dry, their hardness and stiffness are at least twice those of the most competitive engineering polymers and comparable to those of *Glycera* and *Nereis* jaws. Furthermore, the combination of hardness and stiffness makes the beaks more resistant to plastic deformation when in contact with blunt abrasives than virtually all metals and polymers. Their high hardness and stiffness probably reflect a high density of cross-links of both proteins and chitin involving DOPA and possibly His residues. The cross-linkers are also likely responsible for the incomplete chemical analysis. Evidently the bonds are strong enough to prevent release of AAs during acid hydrolysis, thereby precluding further analysis.

The beak microstructure is characterized by a lamellar arrangement of the constituents, with a weak interface that promotes crack deflection and endows the structure with high toughness. The susceptibility of this microstructure to cracking along the lamellae interfaces from contact stresses at the external surfaces is mitigated by the presence of a protective coating. The organization of chitin and proteins within the lamellae is the focus of an ongoing investigation.

The combination of its mechanical properties with its fully organic composition makes the beak tissue an interesting paradigm in structural materials and it may thus serve as an inspiration for the design of similarly robust, wear-resistant synthetic materials.

Acknowledgements

This research was funded by a grant from the National Institutes of Health through the Bioengineering Research Partnership Program (NIHR01DE014672) and a postdoctoral fellowship (A. Miserez) from the Swiss National Science Foundation (PBEL2-104421). This work made use of MRL Central Facilities supported by the MRSEC Program of the National Science Foundation under award No. DMR00-80034. We thank Dr. Cesar Salinas (CIBNOR, La Paz, Mexico) for providing beak samples used in this research.

References

[1] Brooker LR, Lee AP, Macey DJ, Webb J. In: Buschow KH, Flemings MC, Kramer EJ, Cahn RW, Ilschner B, Mahajan S, editors. Encyclopedia of materials: science and technology. Elsevier; 2001. p. 5186–9.
[2] Weiner S, Zaslansky P. In: Buschow KH, Flemings MC, Kramer EJ, Cahn RW, Ilschner B, Mahajan S, editors. Encyclopedia of materials science and technology. Elsevier; 2004. p. 1–5.
[3] Currey JD. J Exp Biol 1999;202:3285–94.
[4] Mann S. Biomineralization: principles and concepts in bioinorganic materials chemistry. New York: Oxford University Press; 2001.
[5] Weiner S, Addadi L, Wagner HD. Mater Sci Eng C 2000;C11:1–8.
[6] Lichtenegger HC, Schöberl T, Bartl MH, Waite H, Stucky GD. Science 2002;298:389–92.
[7] Lichtenegger HC, Schöberl T, Ruokalainen JT, Cross JO, Heald SM, Birkedal H, et al. Proc Natl Acad Sci USA 2003;100:9144–9.
[8] Hillerton JE, Vincent J. J Exp Biol 1982;101:333–6.
[9] Schofield RMS, Nesson MH, Richardson KA. Naturwissenschaften 2002;89:579–83.
[10] Schofield RMS, Nesson MH, Richardson KA, Wyeth P. J Insect Physiol 2003;49:31–44.
[11] Waite H, Lichtenegger HC, Stucky GD, Hansma P. Biochemistry 2004;43:7563–662.
[12] Kear AJ. J Mar Biol Ass UK 1994;74:801–22.
[13] Voight JR. J Zool 2000;252:335–41.
[14] Clarke MR. Nature 1962:560–1.
[15] Clarke MR, editorHandbook for the identification of cephalopod beaks. Oxford: Clarendon Press; 1986.
[16] Gröger J, Piatkowski U, Heinemann H. Polar Biol 2000;23:40–74.
[17] Hernandez-Garcia V. In: Warnke K, Jeupp H, Boletzky SV, editors. Coleid cephalopods through time. Proc Conf. Berlin, Germany: Berliner Paläobiology Abhandlung; 2003.
[18] Nixon M. J Zool 1969;159:363–79.
[19] Nixon M. J Zool 1969;159:451–62.
[20] Castro-Hernandez JJ, Hernandez-Garcia V. Sci Mar 1995;59:347–55.
[21] Jackson GD, McKinnon JF. Polar Biol 1996;16:227–30.
[22] Martinez P, Sanjuan A, Guerra A. Mar Biol 2002;141:131–43.
[23] Hernandez-Lopez JL, Castro-Hernandez JJ, Herandez-Garcia V. Fish Bull 2001;99:679–84.
[24] Roper CFE, Sweeney MJ, Nauen CE. An Annotated and Illustrated Catalogue of Species of Interest to Fisheries, Cephalopods of the World, vol. 3. UN-FAO.
[25] Roper CFE, Mangold K. Systematic and Distributional Relationships of Illex. Cephalopoda: Ommastrephidae: FAO-UN.
[26] Markaida U, Sosa-Nishizaki O. J Mar Biol Ass UK 2003;83:507–22.
[27] Croxall JP, Prince PA. Philosophical Transactions of the Royal Society of London, Series B: Biological Sciences 1996;351:1023–43.
[28] Smale MJ. Philosophical Transactions of the Royal Society of London, Series B: Biological Sciences 1996;351:1067–81.
[29] Hunt S, Nixon M. Comparative Biochemistry and Physiology B-Biochemistry and Molecular Biology 1981;68:535–46.
[30] Hunt S. Polysaccharide–protein complexes in invertebrates. London: Academic Press; 1970, 329.
[31] Jeuniaux C. In: Florkin M, Stotz EH, editors. Comprehensive Biochemistry. Amsterdam: Elsevier Publishing Company; 1971. p. 595–632.
[32] Jeuniaux C. Chitine et Chitinolyse. Un chapitre de la biologie moléculaire, Masson et Cie, Paris; 1963, 181.
[33] Lawn B. Fracture of brittle solids. second ed. Cambridge: Cambridge University Press; 1993, 378.
[34] Hammersley AP. ESRF Internal Report, ESRF97HA02T, FIT2D: An Introduction and Overview, 1997.
[35] Zhao H, Sun C, Stewart RJ, Waite JH. J Biol Chem 2005;280:42938–44.
[36] Gaill F, Persson J, Sugiyama J, Vuong R, Chanzy H. J Struct Biol 1992;109:116–28.
[37] Oliver WC, Pharr GM. J Mater Res 1992;7:1564–83.
[38] Tada H. The Stress Analysis of Cracks Handbook. second ed. St. Louis, MO: Paris Production Inc; 1985.
[39] Kim SS, Kim HK, Lee ML. J Polym Sci Part B: Polym Phys 1996;34, 2637–2374.
[40] Takai M, Shimizu Y, Hayashi J. In: Skjak-Braek G, Anthonsen T, Sandford P, editors. Chitin and Chitosan. Proceedings from the 4th International Conference on Chitin and Chitosan, Trondheim, Norway, August 22–24, 1988. London: Elsevier Science; 1989.
[41] Cullity BD, Stock SR. Elements of X-ray diffraction. Upper Saddle River, NJ: Prentice Hall; 2001, 664.
[42] Koch MHJ, Vachette P, Svergun DI. Q Rev Biophys 2003;36:147–227.
[43] Broomell C, Khan R, Mattoni M, Waite JH, Stucky GD, Zok F. J Exp Biol, in press.
[44] Johnson KL. Contact mechanics. Cambridge: Cambrige University Press; 1985.
[45] Bushan B. Principles and applications of tribology. New York: John Wiley & Sons; 1999, 1020.

[46] Lawn B. J Am Cer Soc 1998;81:1977–94.
[47] Lawn B. Proc R Soc London A 1967;299:307–16.
[48] Vincent JFV, Wegst U. Arthropod Struct Dev 2004;33:187–99.
[49] Wainwright SA, Biggs WD, Currey JD, Gosline JW. Mechanical design in organisms. Princeton, NJ: Princeton University Press; 1976.
[50] Andersen SO, Hojrup P, Roepstorff P. Insect Biochem 1995;25: 153–76.
[51] Iconomidou VA, Willis JH, Hamodrakas SJ. Insect Biochem 2005; 35:533–60.
[52] Kerwin JL, Whitney DL, Sheikh A. Insect Biochem Molec Biol 1999;268:599–607.
[53] Kramer EJ, Kanost MR, Hopkins TL, Jiang H, Zhu YC, Xu R, et al. Tetrahedron 2002;57:385–92.
[54] Willis JH, Iconomidou VA, Smith VF, Hamodrakas SJ. In: Gilbert L, Iatrou K, Gill S, editors. Comprehensive molecular insect science. Oxford: Elsevier; 2005. p. 79–110.
[55] Moses DN, Mattoni M, Slack NL, Waite H, Zok F. Acta BioMaterialia 2006;2:521–30.
[56] Birkedal H, Khan RK, Slack NL, Broomell C, Lichtenegger HC, Zok F, et al. Chem Bio Chem 2006;7:1392–9.
[57] Sugumaran M. In: Binnington K, Retnakaran A, editors. Physiology of the insect epidermis. Melbourne: CSIRO Publications; 1991. p. 141–68.
[58] Waite JH. Comp Biochem Physiol B Biochem Mol Biol 1990;97:19–29.
[59] Zhao H, Waite JH. Biochemistry 2005;44:15915–23.
[60] Koch AW, Holstein TW, Mala C, Kurz E, Engel J, David CN. J Cell Sci 1998;111:1545–54.
[61] Lichtenegger HC, Birkedal H, Casa DM, Cross JO, Heald SM, Waite JH, et al. Chem Mater 2005;17:2927–31.
[62] Miserez A, Robertson N, Schneberk T, Sun C, Zok F, Waite H. in preparation.
[63] Carlstrom D. J Biophys Biochem Cytol 1957;3:669–83.
[64] Blackwell J. Biopolymers 1969;7:281–98.